การประชุมวิชาการเครือข่ายวิศวกรรมเครื่องกลแห่งประเทศไทยครั้งที่ 19
19-21 ตุลาคม 2548 จังหวัดภูเก็ต

# Case Study of Finite Element Method and Photoelasticity for Contact Mechanics Problems

[1]วิโรจน์ ลิ่มตระการ
[2]บรรจง เดชาพานิชกุล
[3]สุธี โอฬารฤทธินันท์
[4]สุวัฒน์ จีรเธียรนาถ
[1,2]ภาควิชาวิศวกรรมเครื่องกล คณะวิศวกรรมศาสตร์ มหาวิทยาลัยธรรมศาสตร์ ศูนย์รังสิต
99 หมู่ 18 แขวงคลองหนึ่ง เขตคลองหลวง ปทุมธานี 12120
โทร 0-25643001 ต่อ 3144 โทรสาร 0-25643001 ต่อ 3049 E-mail: limwiroj@engr.tu.ac.th
[3, 4]ศูนย์เทคโนโลยีโลหะและวัสดุแห่งชาติ
114 ถนนพหลโยธิน ต. คลองหนึ่ง อ. คลองหลวง จ. ปทุมธานี 12120

[1]Wiroj Limtrakarn
[2]Bunjong Dechapanichkul
[3]Sutee Olarnrithinun
[4]Suwat Jirathearanat
[1,2]Department of Mechanical Engineering, Faculty of Engineering, Thammasat University, Rangsit Campus
99 Moo 18, Klong Luang, Pathumthani 12120 Thailand
Tel: 0-25643001 Ext. 3144 Fax: 0-25643001 Ext. 3049 E-mail: limwiroj@engr.tu.ac.th
[3]National Metal and Materials Technology Center
114 Paholyotin Road, Klong 1, Klong Luang, Pathumtani Province 12120 Thailand

**Abstract**

The Finite element method and photoelasticity technique are presented to predict the stress distribution for contact mechanics problems. The paper first describes 2D contact mechanics theory. Next, the finite element formulations based on the combination of Lagrange multiplier and Penalty method are presented, The computational procedure and its boundary conditions are then represented. The photoelasticity theory and its procedure are also explained. To assess the validation and efficiency of both techniques, the displacement and stress distributions for two circular plates contact problem and circular–flat plate contact problem will be predicted by using finite element method and compared to those results gained from photoelasticity technique and analytical solutions. The solutions show that the stress distributions predicted by finite element method are in good agreement with the photoelasticity and analytical results.

## 1. Introduction

In solid mechanics problems, the contact condition between two surfaces is one of important factors that affects the maximum stress in static loading or wear in dynamic loading. A correct understanding in the contact behavior under static loading can be directly implemented on the product design and can be extended to use with the contact behavior under dynamic loading such as sheet metal stamping process. The finite element method is employed to predict the contact behavior for several years. Consequently, there are many finite element algorithms invented to predict the contact behavior in static loading such as Penalty algorithm, Lagrange multiplier algorithm and augmented Lagrange multiplier, and etc.

This paper studied the capability and performance of contact algorithms for solving 2D contact problems. The finite element method for 2D contact mechanics is presented. The computational procedure and its boundary conditions are shown. Two contact algorithms (Penalty algorithm and Lagrange multiplier algorithm) are used in displacement and stress distribution analysis for two deformable circles contact together and a deformable circle contact with deformable rectangular plate. Then, the computational results are validated with analytical solution and photoelasticity.

## 2. Theory

### 2.1 Governing differential equation

Contact mechanics is governed by the equilibrium equations, strain–displacement relations and constitutive equations.

2.1.1 Equilibrium equations

The equilibrium equations can be written in variational form as [1],

$$\delta W_S - \delta W_R - \delta W_C = \int_\Omega \sigma_{ij} \delta e_{ij} d\Omega - \int_S t_i \delta u_i dS = 0 \quad (1)$$

where $\delta W_S$, $\delta W_R$ and $\delta W_C$ are virtual energy of internal stress, external force and contact, respectively. $\sigma_{ij}$, is the stress components, $\delta e_{ij}$ is virtual strain, $t_j$ is the surface traction, and $\delta u_i$ is virtual displacement. Boundary conditions may consist of specifying the surface traction [2] as depicted in Fig. 1 as,

$$\sigma_{ij} n_i = t_1 \quad (2)$$

where $n_i$ and $t_1$ are the outward unit normal vector and surface traction on the boundary $S_1$ at time t, respectively. The boundary condition may include the prescribed displacement on the boundary $S_2$ as,

$$u_i(x,t) = u_2(t) \quad (3)$$

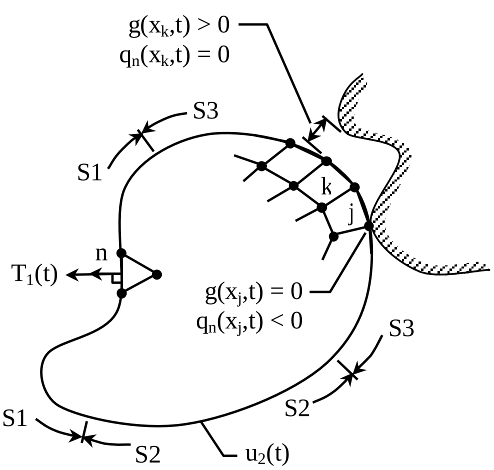


Figure 1 – Boundary conditions for contact mechanics problem.

Also along the contact boundary $S_3$, the normal contact stress should be compressive and the boundary should not penetrate into the other as follows,

$$q_n(x,t) = q_c(x,t)\, n_i = 0 \quad (4)$$

$$g(x,t) = g(x) - u(x,t)\, n_i = 0 \quad (5)$$

where $q_c(x,t)$ is the contact traction, $q_n(x,t)$ is the normal component of contact traction, and $g(x,t)$ is the gap between the two boundary surfaces.

The equation 4 and 5 are the contact conditions of Lagrange multiplier method. This method expresses the virtual work in the form,

$$\delta W_C = \int_S \delta\left(\lambda_N g_N + \lambda_T g_T\right) dS \quad (6)$$

where $\lambda$ is the Lagrange multiplier and equivalent to the reaction force at contact point.

The other contact algorithm is Penalty method. It will allow very small penetration occurs on contact surface.

$$g(x,t) = g(x) - u(x,t)\, n_i = 0 \quad (7)$$

$$\delta W_C = \int_S \left(\varepsilon_N g_N \delta g_N + t_T \delta g_T\right) dS \quad (8)$$

where $\varepsilon$ is the Penalty parameter, subscript N and T mean normal and tangential direction, respectively. Equation 8 is valid under slip condition. If the contact condition is pure stick then $t_T = \varepsilon_T\, g_T$.

2.1.2 Strain-displacement relations

Contact behavior will occurs small strain and normally considered the strain-displacement relations in the form,

$$\varepsilon_{ij} = \frac{1}{2}\left(u_{i,j} + u_{j,i}\right) \quad (9)$$

where $\varepsilon_{ij}$, is the strain components; $u_i$, and $u_j$, are the displacement components.

2.1.3 Constitutive equations

Contact mechanics has the constitutive equation that shows the relation of elastic strain, $\varepsilon_{ij}$ and the elastic stress, $\sigma_{ij}$ in the form,

$$\{\sigma\} = [C]\{\varepsilon\} \quad (10)$$

where $[C]$ is the elasticity matrix [3].

## 2.2 Finite Element Equations

The weak form of virtual work principle [2] is applied to the equilibrium equation 1 and written in matrix form as,

$$[K]\{U\} = \{F\} + \{F_C\} \quad (11)$$

where $[K]$ is the stiffness matrix, $\{U\}$ is the displacement vector, $\{F\}$ is the external load vector, and $\{F_C\}$ is the load vector of contact force.

## 2.3 Photoelasticity [4, 5]

Photoelasticity technique can be explained with the wave theory of light in the form of harmonic waveform.

$$E = A \cos\left(\phi - \omega t\right) \quad (12)$$

where E is magnitude of light wave, A is the wave amplitude, $\phi$ is the phase angle of wave, $\omega$ is angular frequency, and t is time.

$$\phi = \frac{2\pi}{\lambda}(z+\delta) \tag{13}$$

$$\omega = 2\pi f = \frac{2\pi v}{\lambda} \tag{14}$$

where z is position along propagation axis, $\lambda$ is wavelength, $\delta$ is phase of wave, f is wave frequency and v is wave velocity.

Photoelasticity technique will control light path from source through wave plates and measured model is located in the middle of them as shown in figure 2.

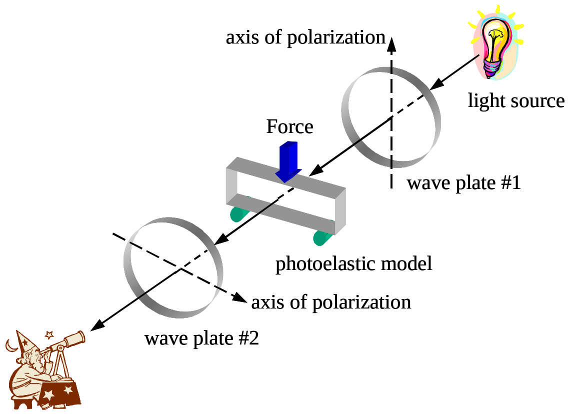


Figure 2 – A photoelastic model in a plane optical components.

A wave plate resolve an incident light wave into parallel and perpendicular to the axis of polarization. The parallel component is transmitted, and the other component is internally absorbed.

After light wave entering photoelastic model under loading, the stressed model exhibits the optical properties of a wave plate. The incident light wave is resolved into parallel and perpendicular to the principal stress directions at the point. After leaving the photoelastic model, the two component with different velocities enter the wave plate #2 and are resolved again.

The leaving light wave has a relative retardation or angular phase shift, $\Delta$ in the following equation.

$$\Delta = \frac{2\pi}{\lambda}\delta = \frac{2\pi h}{\lambda}(n_2 - n_1) \tag{15}$$

where h is the wave plate thickness, and n is the refractive index of media.

The principal stresses is related to the refractive index in the form,

$$n_2 - n_1 = c(\sigma_1 - \sigma_2) \tag{16}$$

Equation 18 is called stress–optic law. c is the relative stress–optic coefficient), $\sigma_1$ and $\sigma_2$ are the major and minor principal stress, respectively.

After substituting equation 16 into equation 15, the equation is in the form,

$$\sigma_1 - \sigma_2 = \frac{N f_\sigma}{h} \tag{17}$$

where N is the number of fringes appearing in an isochromatic fringe pattern and $f_\sigma$ is the material fringe value.

$$N = \frac{\Delta}{2\pi} = \frac{\delta}{\lambda} \tag{18a}$$

$$f_\sigma = \frac{\lambda}{c} \tag{18b}$$

## 3. Examples

This paper focuses on two contact algorithms for finite element analysis, Penalty method and Lagrange multiplier method. The efficiency of each method is studied and compared with analytical solutions in two examples. The examples used in this paper are two circular plates contact problem and circular–flat plate contact problem.

### 3.1 Two circular plates contact problem

As shown in figure 3, two deformable circles contact together. Force 110.8 N is applied on the top circle while the bottom circle lies on the rigid floor. Both circles have the same material properties and dimension ie.Young's Modulus E = 952.889 MPa, Poisson's ratio = 0.38 and radius = 25 mm.

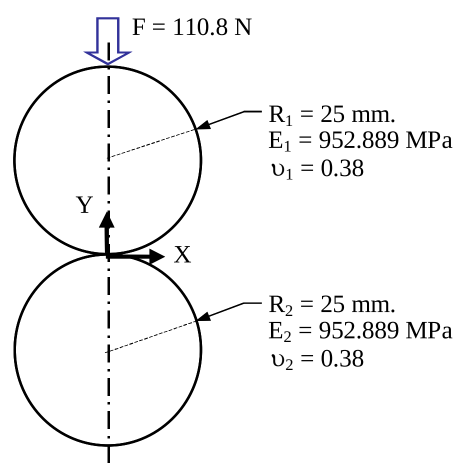


Figure 3 – Two circle plate contact problem statement.

The contact behavior between two circles is investigated and has the solution based on Hertz theory in the form,

$$a = 2\sqrt{\frac{F}{l}\cdot\frac{1}{\pi}\cdot\frac{\left(1-\nu_1^2\right)/E_1+\left(1-\nu_2^2\right)/E_2}{1/R_1+1/R_2}} \qquad (19a)$$

$$b = 0.638\frac{F}{l}\cdot\left(\frac{1-\nu_1^2}{E_1}\right)\cdot\left[\frac{2}{3}+\ln\frac{2R_1}{a}+\ln\frac{2R_2}{a}\right] \qquad (19b)$$

where a is the contact length and b is the displacement of top circular plate in y direction.

The finite element model consists of 5,360 nodes and 5,280 elements for half right model. Figure 7 shows detail of elements near contact surface.

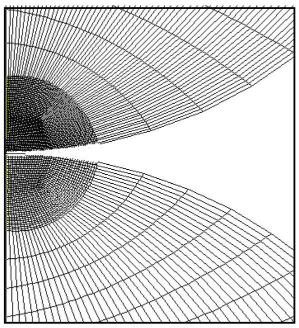

Figure 4 – Finite element model around contact surface.

Applied forces are set at 27.7 N, 55.4 N, 83.1 N, and 110.8 N following force scale of photoelasticity equipment. The deformation solution is compared with Hertz theory. Figure 5 shows the relation of contact length and applied forces. The solution error of the Penalty method is 0.7%, which much less than that of Lagrange multiplier method (10%). Figure 6 displays displacement along y axis depending on applied force. When comparing the solutions with hertz theory, Penalty and Lagrange multiplier show the proximate level of accuracy.

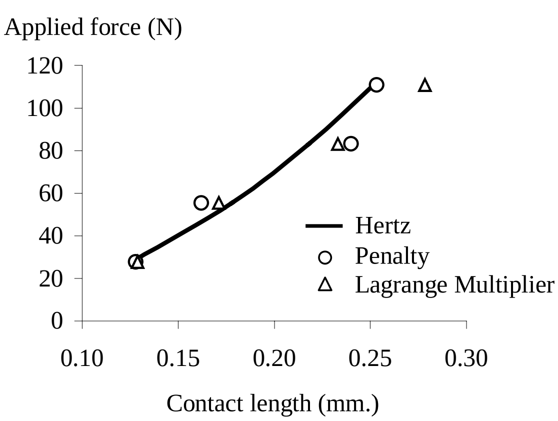


Figure 5 – Plot of applied force and contact length.

Although, the more accuracy of solution can be obtained by reducing the element size around the contact surface, however, the smaller element size, the more expense in CPU time and space storage are required.

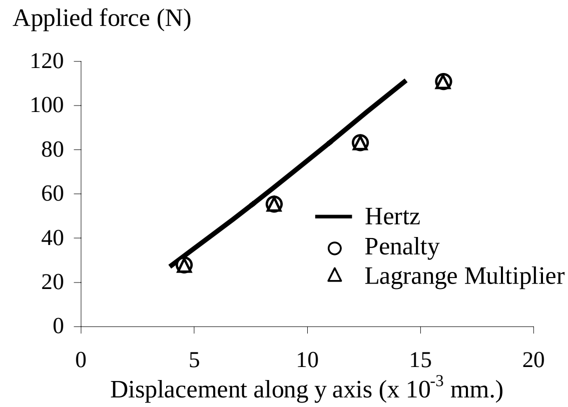


Figure 6 – Plot of applied force and displacement in y axis.

For stress analysis, the solutions from both Penalty and Lagrange multiplier method are the same. Figure 7 expresses the normal stress and distance in y direction. Figure 8 displays the normal stress y along the circumference.

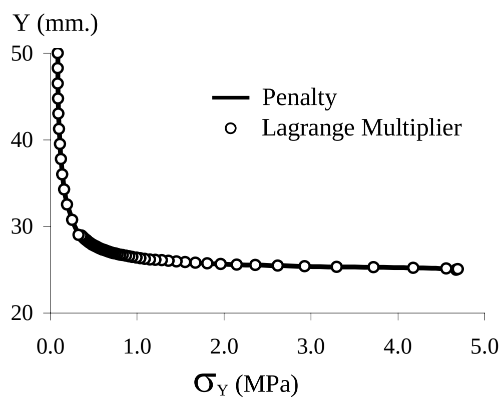


Figure 7 – Plot of normal stress y along y axis.

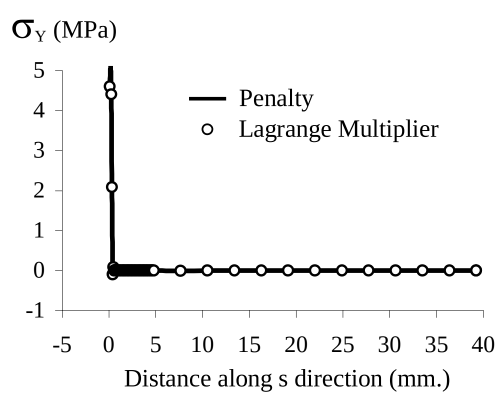


Figure 8 – Plot of normal stress y along s direction.

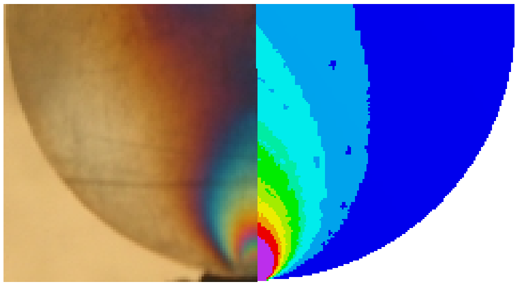

Photoelasticity Finite Element Method

Figure 9 Comparison of max shear stress between photoelasticity result and finite element method solution.

Figure 9 shows the maximum shear stress contours of the photoelasticity result and finite element solution based on 110.8 N applied on the top circle. As the result suggested, both results have a good agreement.

3.2 Circular–flat plate contact problem

A circular plate is applied force in y direction and contacts a deformable flat plate as shown in figure 10. Because of symmetry, the finite element model is generated only the right half of the model and consists of 5,580 nodes and 5,450 elements.

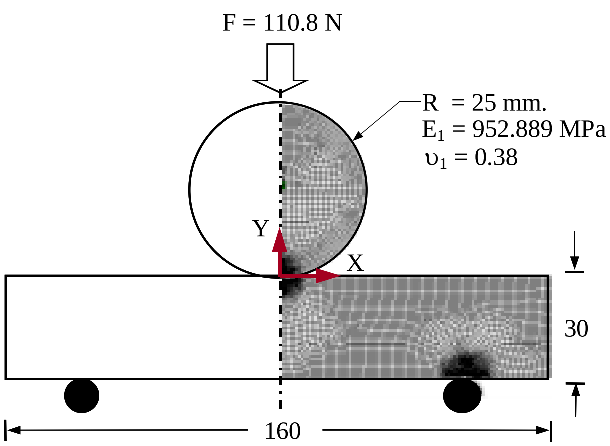


Figure 10 – Circular–flat plate contact problem statement.

Stress and displacement behavior near the contact surface are based on contact mechanics theory, while the behavior at the bottom edge of flat plate is based on bending theory.

The finite element solution agrees well with the result from photoelasticity technique as shown by maximum shear stress contours in figure 11.

According to the results of the Penalty and Lagrange multiplier method, the accuracy of both methods is equally the same as shown in figure 12–15.

Contact lengths and displacement along y axis will increase as the applied forces increasing as shown in figure 12 and 13.

The maximum normal stress in the y direction will occur at a contact point (y = 0 mm.) and will decrease when the distance is far away as shown in figure 14 and 15.

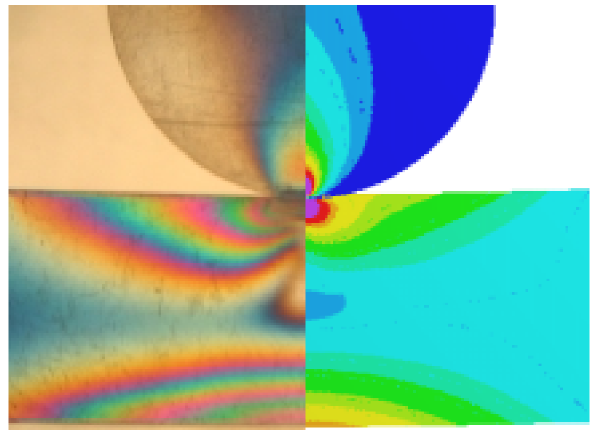

Photoelasticity Finite Element Method

Figure 11 – Comparison of max shear stress between photoelasticity result and finite element method solution.

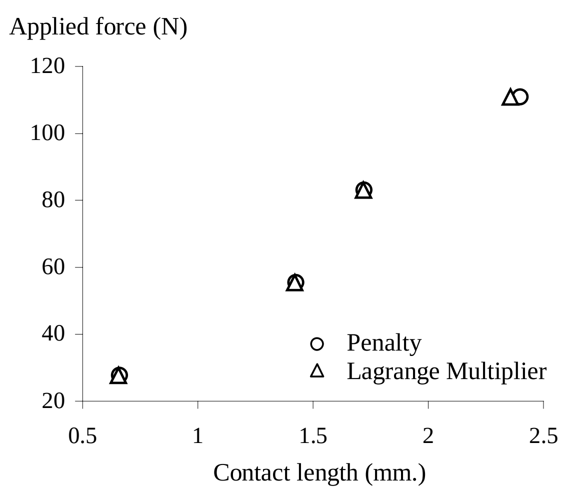


Figure 12 – Plot of applied force and contact length

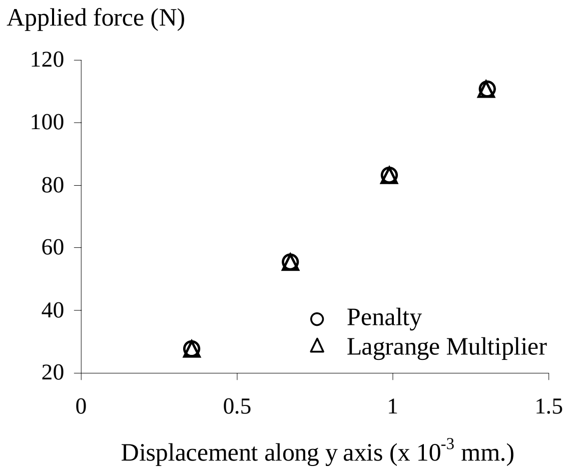


Figure 13 – Plot of applied force and displacement in y axis.

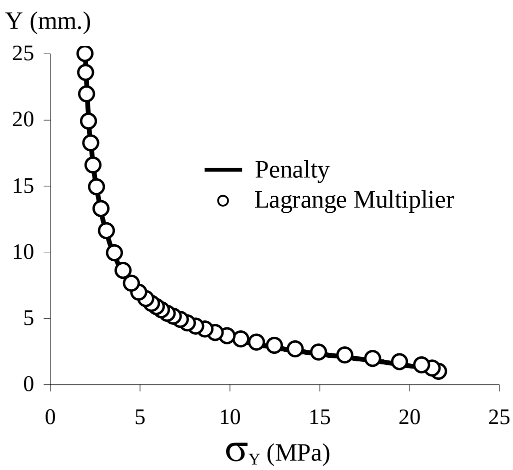


Figure 14 – Plot of normal stress y along y axis.

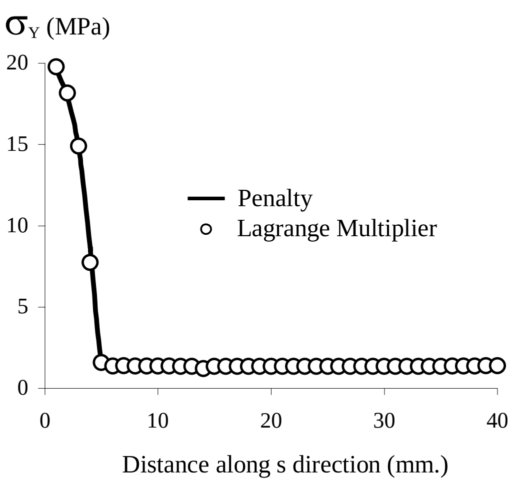


Figure 15 – Plot of normal stress y along s direction.

## 4. Conclusions

This paper presents the finite element method and photoelasticity method for solving the contact mechanics problem. Case studies are two circular plate contact problem and circular–flat plate contact problem. Results show that the Penalty and Lagrange multiplier method can be used to predict the contact behavior efficiently. Computational results are compared with the Hertz theory and photoelasticity result and have a good agreement.

## 5. Acknowledgements

The author is pleased to acknowledge Thailand Graduate Institute of Science and Technology (TGIST) and National Metal and Materials Technology Center (MTEC) for supporting this research work.

## 6. References

1. Fung, Y. C., Foundations of Solid Mechanics, International Edition, Prentice-Hall, 1965.
2. Zhong, Z. H., Finite Element Procedures for Contact-Impact Problems, Oxford University Press, Oxford, 1993.
3. Zienkiewicz, O. C. and Taylor, R. L., The Finite Element Method, Fourth Ed., Vol. I, McGraw-Hill Press, Singapore, 2004.
4. Dally, J. W. and Riley, W. F., Experimental stress analysis, Third edition, Singapore, McGraw–Hill, 1991.
5. Limtrakarn, W., “Comparison in the stress analysis of 2D solid mechanics problems of finite element method and photoelasticity”, KMUTT Research and Development Journal, Vol. 28, No.1, 2005.
6. Dechaumphai, P. Finite Element Method in Engineering, Third Ed., Chulalongkorn University Press, Bangkok, Thailand, 2004.
7. Wriggers, P., “Computational contact mechanics”, John Wily & Sons, 2002.